JOURNAL OF GEOPHYSICAL RESEARCH, VOL. 88, NO. C10, PAGES 5960–5972, JULY 20, 1983

Near-Inertial Motions Off the Oregon Coast

IAIN ANDERSON

United States Coast Guard, Atlantic Area, Governors Island, New York 10004

ADRIANA HUYER AND ROBERT L. SMITH

School of Oceanography, Oregon State University, Corvallis, Oregon 97331

Near-inertial motions were observed at all current meters in an array of five moorings spanning the continental margin off central Oregon during October 1977 to January 1978. All moorings were between 10 and 130 km from shore, in water depths between 100 m and 2500 m. Largest near-inertial amplitudes (>30 cm/s) were observed at the uppermost current meters of the offshore moorings, although these were below the surface mixed layer. The near-inertial energy generally decreased with increasing depth, and there was less near-inertial energy over the continental shelf than at similar depths offshore. The energy levels observed over the shelf were about the same as observed there during summer 1973, and the energy levels observed offshore were comparable with those observed in the open North Atlantic. Horizontal coherence scales were large, exceeding 115 km during the first half of the observational period and about 60 km during the second half; estimates of the horizontal wavelength (50 km during the first half and 20 km during the second half) suggest that the coherence scale is of the order of three wavelengths. Although we did not have current data in the surface mixed layer nor wind measurements over each mooring, the available meteorological data (synoptic pressure charts and hourly wind and pressure at Newport) suggest that most of the near-inertial energy was forced by the local wind.

INTRODUCTION

Pure inertial motion on the rotating earth is circular, rotating clockwise in the northern hemisphere with a period of $2\pi/f$, where f is the local Coriolis parameter. Such pure inertial motions are seldom observed in the ocean. There is almost always some other force acting on the fluid that cannot be completely neglected. However, motions that are very nearly inertial in character (called 'near-inertial motions') with very nearly circular rotation in the proper sense and with a frequency near f have been observed at all depths in the oceans and large lakes of the world [*Webster*, 1968]. The most common characteristics of near-inertial motions are well documented [*Kroll*, 1975; *Kundu*, 1976; *Fu*, 1981; *Thomson and Huggett*, 1981]. They are highly intermittent and generally last only a few oscillations with a maximum velocity of 20–30 cm/s; the observed frequency, ω, is generally slightly greater than f; vertical coherence scales are of the order of only a few tens of meters; and horizontal coherence scales are of the order of a few tens of kilometers.

Previous studies of inertial currents have usually been conducted either in the open ocean [e.g., *Pollard*, 1980; *Fu*, 1981] or over the continental shelf [e.g., *Johnson*, 1976; *Thomson and Huggett*, 1981]. The few available studies of near-inertial motions over the Oregon shelf are based exclusively on data collected in summer. Maximum amplitudes observed over the Oregon shelf were about 15 cm/s during the summer of 1973 [*Johnson*, 1976; *Kundu*, 1976], considerably lower than the open-ocean surface-layer values of about 50 cm/s at site D in the North Atlantic [*Pollard*, 1980] and 35 cm/s in the Mediterranean [*Gonella*, 1971]. Horizontal coherence scales over the Oregon shelf were between 10 and 35 km during summer 1972 [*Kindle*, 1974] and about 15 km during summer 1973 [*Johnson*, 1976]; these are small in comparison with horizontal coherence scales of about 60 km in the North Atlantic [*Pollard*, 1980; *Fu*, 1981].

In this paper, we investigate near-inertial motions in current observations made during late fall and winter at five sites spanning the continental margin off central Oregon. We describe the near-inertial motions in terms of their amplitude, coherence, and phase by using both spectral and band-passing techniques, and attempt to account for their generation by the local wind. Where appropriate, the results are compared with those of previous studies.

OBSERVATIONS

During 1977 and 1978, Oregon State University and the University of Washington conducted a joint field program, the Slope Undercurrent Study (SUS), to study the circulation along the continental slope off central Oregon. As part of this study, an array of current meters was moored across the continental margin at 45°20'N between October 1977 and January 1978 (Figure 1). Occasional hydrographic sections were made along the moored array, and coastal winds were measured continuously at Newport, Oregon.

The SUS array consisted of five moorings: 'Skunk,' over the 2600 m isobath just seaward of the foot of the continental slope with current meters at 100, 600, and 1850 m; 'Leopard,' over the 1100 m isobath at midslope with current meters at 70 and 820 m; 'Ocelot,' over the 600 m isobath on the upper slope with current meters at 141, 243, and 371 m; 'Puma,' at the 300 m isobath near the shelf break with current meters at 64, 164 and 261 m; and 'Elephant,' over the 110 m isobath at mid-shelf with current meters at 23, 49, and 89 m. Ocelot and Elephant were maintained by the University of Washington, and Skunk, Leopard, and Puma were maintained by Oregon State University. All moorings were deployed in October, with intended recovery in January, but the original Puma mooring was lost and replaced in November, and Ocelot was recovered prematurely in early December. Although there was only a very brief (390-hour) period with data from all five moorings, there are two

Paper number 3C0480.
0148-0227/83/003C-0480$05.00

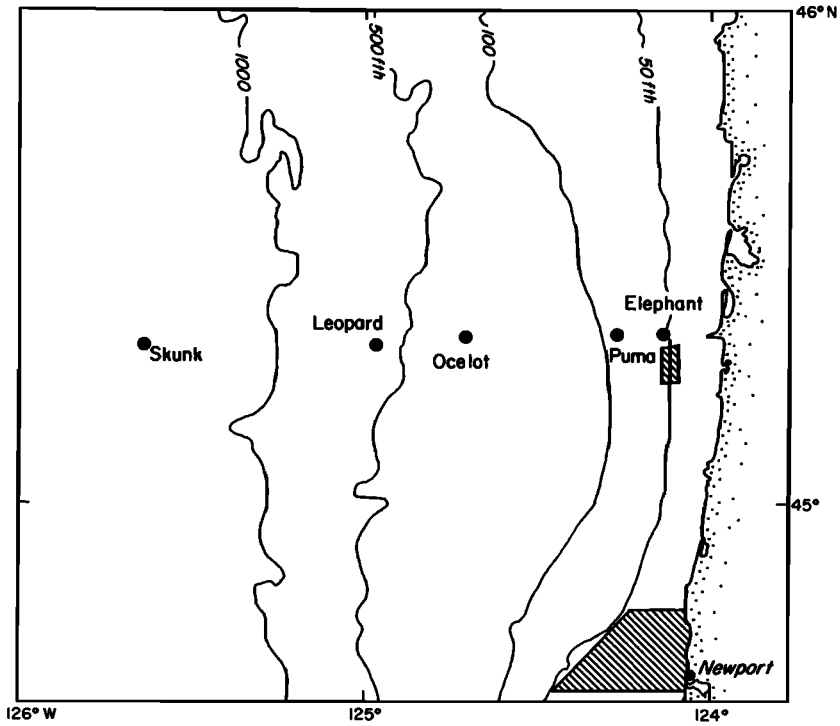

Fig. 1. Location of the moorings of the Slope Undercurrent Study. The shaded areas indicate the location of prior studies of inertial currents.

periods of about 55 days each with data from four separate moorings (Figure 2). These two periods are limited by the duration of Ocelot and Puma, respectively (Figure 2).

All of the moorings of the SUS array were sub-surface, and Aanderaa current meters were used throughout. All instruments recorded mean speed and instantaneous direction at inervals of 40 min. Time series of speed were plotted for error detection, and spurious values were replaced by linear interpolation. After removal of obvious errors, the speed and direction were used to determine the eastward (u) and northward (v) components of the current. Record gaps of 120 hours beginning at 0900 October 10 in Ocelot 371 m and 136 hours beginning at 0200 December 9 in Puma 261 m were were filled with zeroes. The data were filtered with a half power point of 2.5 hours to suppress high frequency signals and decimated to hourly values to yield the processed data.

Vertical profiles of the square of the Brunt-Väisälä frequency, $N^2 = -g\,\partial\rho/\bar{\rho}\,\partial z$ (where ρ is density, g is the acceleration due to gravity, and z is vertically upward), were computed from the hydrographic data by using a centered finite difference of 20 m. These profiles (e.g., Figure 3) show that most of the current meters in the array were below the surface mixed layer, during both the first (Ocelot) and second (Puma) periods. The mixed layer was fairly shallow (less than 25 m) during the first period.

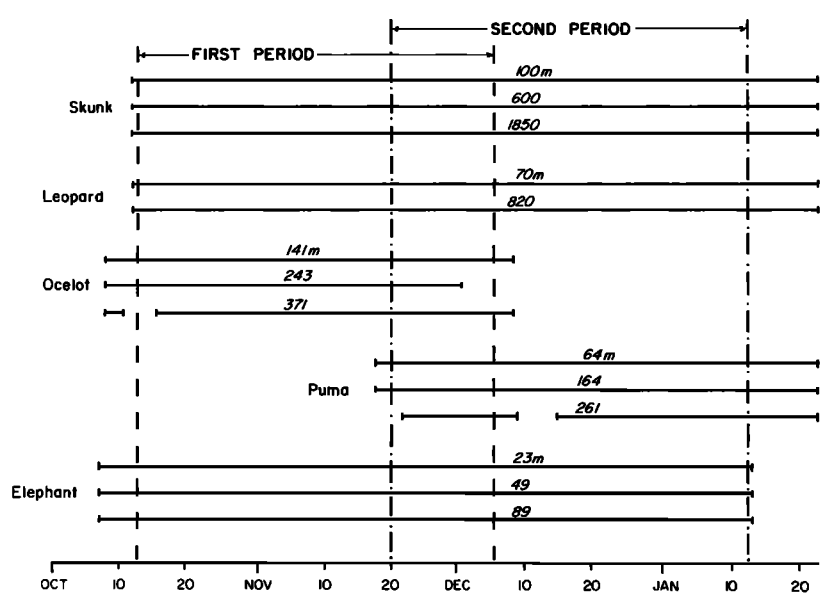

Fig. 2. Summary of the time span of the current meter data. The two time periods used for spectral analysis are indicated.

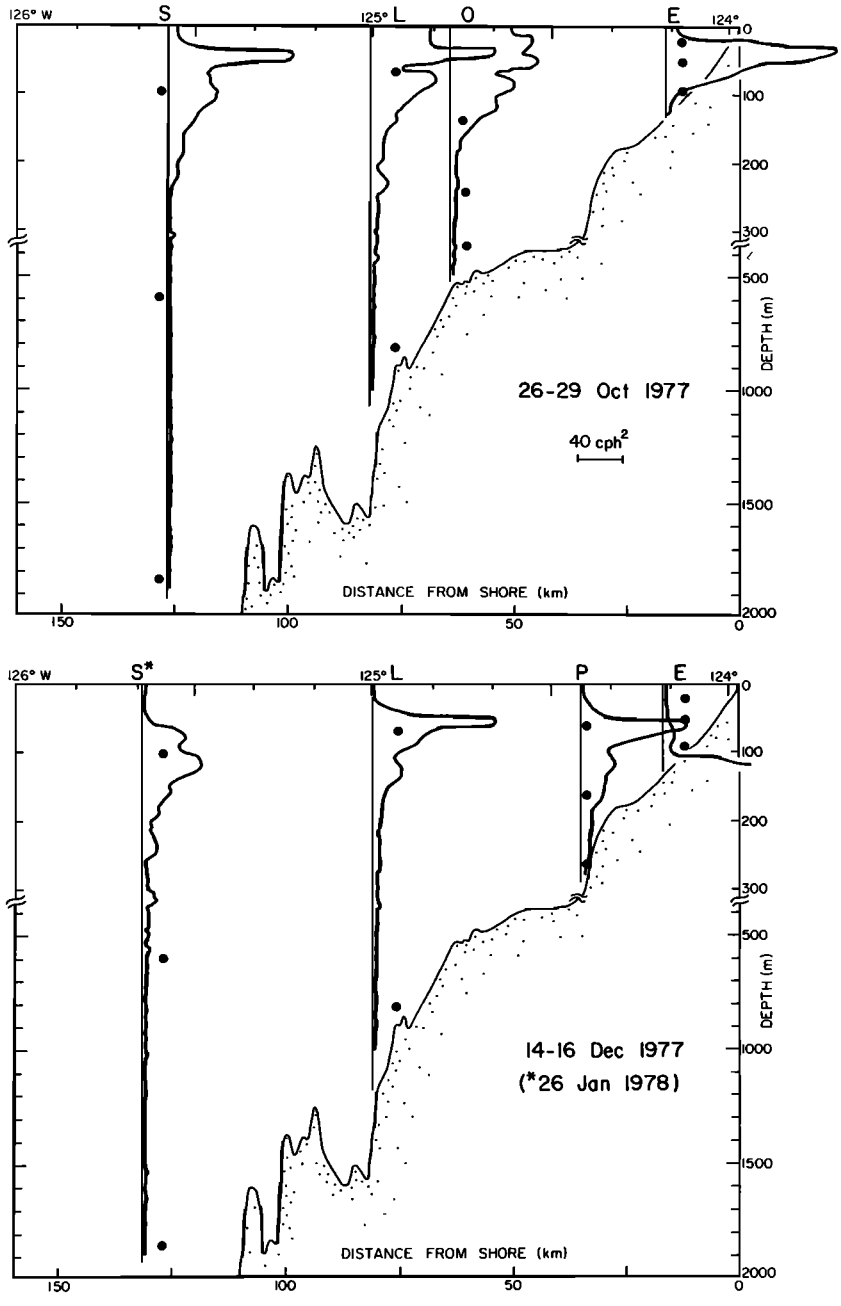

Fig. 3. Profiles of the Brunt-Väisälä frequency, N^2, near each mooring.

The only current meter possibly in the mixed layer was Elephant 23 m; the top current meter of each other mooring was in the pycnocline (Figure 3). During the second period, the mixed layer reached almost to the bottom over the shelf, placing Elephant 23 m and 49 m in the mixed layer and Elephant 89 m in the pycnocline; again, the top current meter of each other mooring was in the pycnocline.

Time series of the eastward component of the current at all current meters (Figure 4) show frequent episodes with motion that has a period of about two-thirds of a day (i.e., roughly the local inertial period of 17 hours). Some of these episodes appear to begin impulsively (e.g., at Leopard 70 m on December 13), but others show a gradual increase in amplitude (e.g., at Leopard 70 beginning about October 25). The amplitude of these oscillations appears to decrease with depth at all moorings (Figure 4). Although only the upper current meters at Elephant are in the surface mixed layer, all of the current records from the SUS array contain a substantial amount of near-inertial motion.

Spectral Analysis

The vector time series from each current meter were used to calculate rotary spectra, which separate the clockwise- and counterclockwise-rotating frequency components [*Mooers*, 1973]. Pure inertial motion at this latitude would have a clockwise-rotating peak at 0.0592 cph and no counterclockwise energy. Since the common record length for all five moorings was too short for meaningful spectral analysis, we used two time periods of 1280 hours, which both had simultaneous data

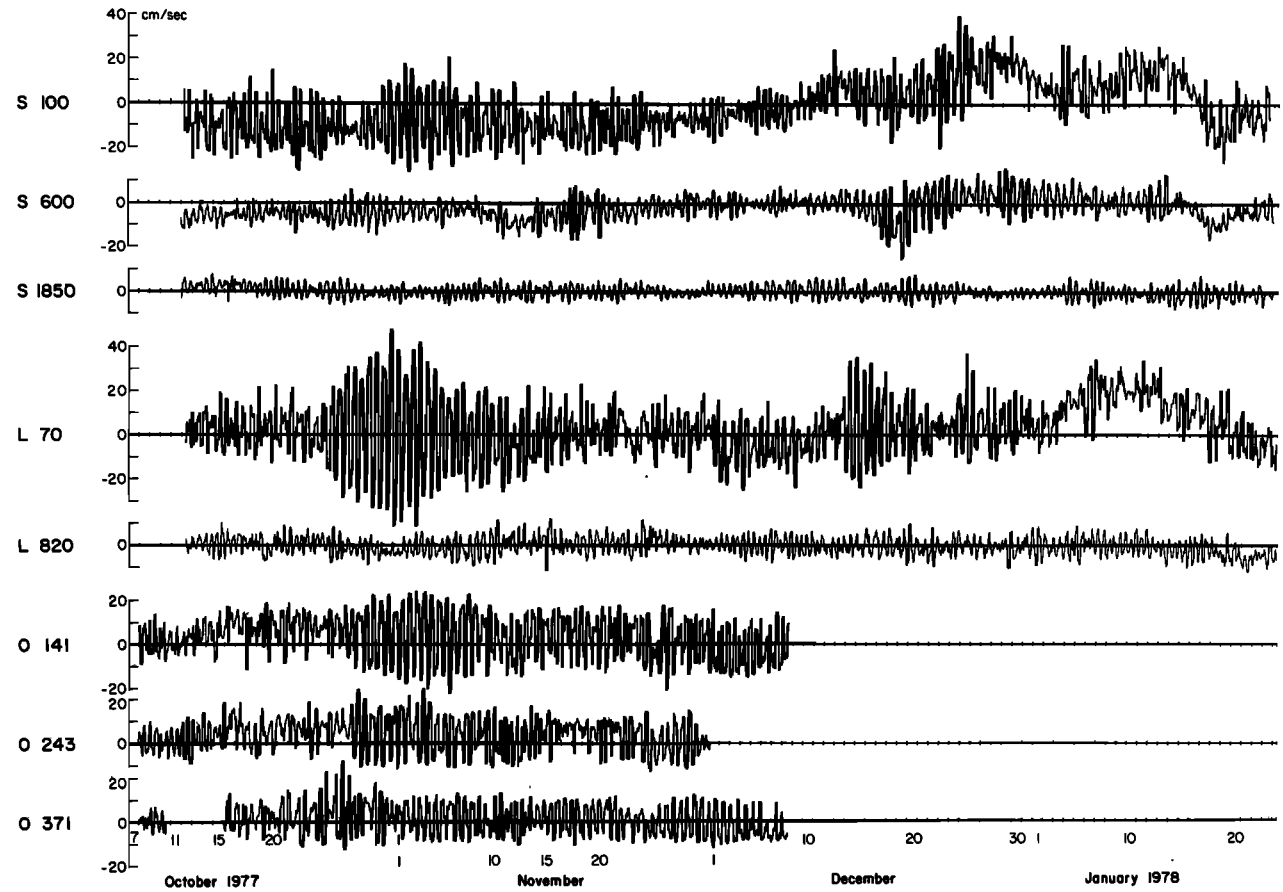

Fig. 4*a*

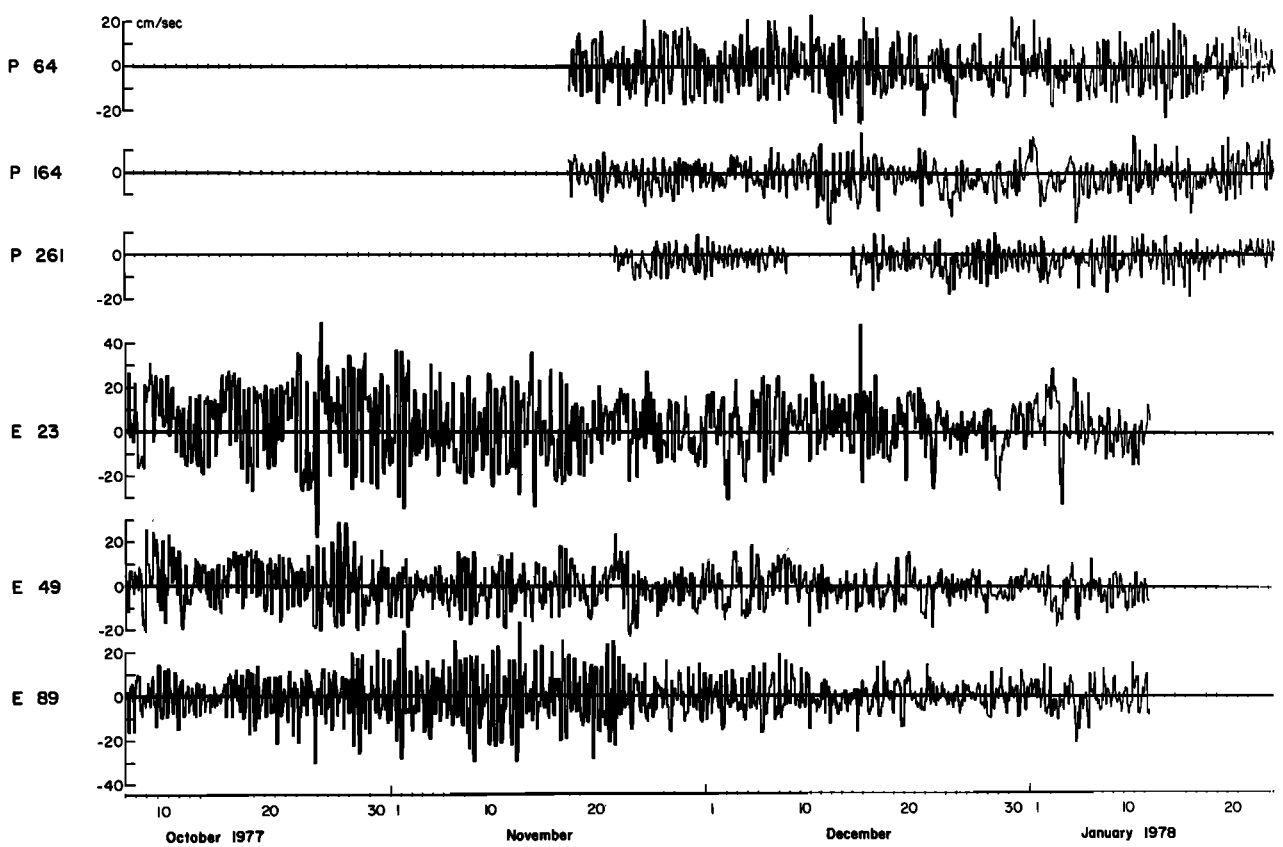

Fig. 4*b*

Fig. 4. The eastward (*u*) components of the currents at the current meters at (*a*) Skunk, Leopard, and Ocelot, and (*b*) Puma and Elephant.

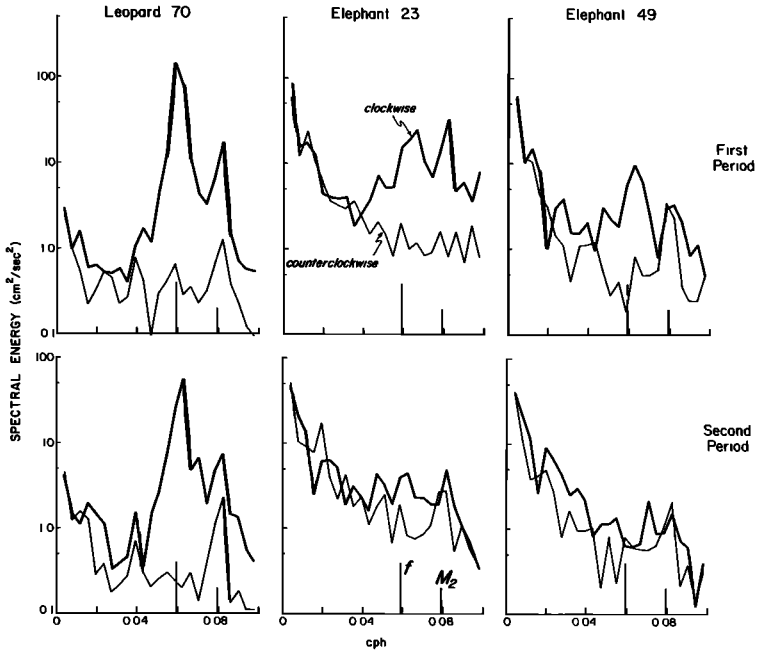

Fig. 5. Rotary spectra of selected current meter records for both the first (Oct. 13 to Dec. 5) and second (Nov. 20 to Jan. 12) time periods. The local inertial frequency f, and the semidiurnal frequency M_2 are indicated.

from four of the moorings (Figure 2). The first time period, with data from Skunk, Leopard, Ocelot, and Elephant, began at 0400 UT October 13 and ended at 1200 UT December 5; this period included an episode of strong near-inertial motion at the end of October. The second period started at 0400 UT November 20, ended 1200 UT January 12, and included data from Skunk, Leopard, Puma, and Elephant. We allowed the two periods to overlap by 15 days to use as much of the available data as possible. Spectra were obtained for each time period by ensemble-averaging five periodograms calculated from 256-hour record segments. The resulting spectra have 10 degrees of freedom and a spectral bandwidth of 0.0039 cph, about 6% of f.

The rotary autospectra for the first time period (e.g., Figure 5) all show a prominent clockwise-rotating peak near the local inertial frequency and very little counterclockwise energy in that frequency band. In all cases, the near-inertial energy is equal to or greater than the semi-diurnal energy. The peak frequency of the near-inertial motion varies slightly among the different current meters; in most cases, it is somewhat greater than f. Similar frequency shifts have been observed elsewhere in the ocean [e.g., *Fu*, 1981; *Gonella*, 1971; *Kundu*, 1976]. The peak energy decreases with increasing depth at each location except over the continental shelf (Table 1, Figure 6). The ratio between the major and minor axes computed from the rotary

TABLE 1. Characteristics of the Clockwise Near-Inertial Peak in the Rotary Spectrum for Each Current Meter During Both Time Periods

	First Period (Oct. 13 to Dec. 5)				Second Period (Nov. 20 to Jan. 12)			
Current Meter	Peak Energy, cm^2/s^2	Peak Frequency, cph	Width cph	Major Axis/ Minor Axis	Peak Energy, cm^2/s^2	Peak Frequency, cph	Width cph	Major Axis/ Minor Axis
S 100 m	26.9	0.0625	0.0098	1.01	19.9	0.0586	0.0106	1.01
S 600 m	5.1	0.0625	0.0085	1.01	11.3	0.0586	0.0097	1.02
S 1850 m	1.9	0.0625	0.0066	1.02	2.7	0.0625	0.0101	1.02
L 70 m	147.0	0.0586	0.0060	1.01	56.1	0.0625	0.0054	1.00
L 820 m	3.4	0.0625	0.0062	1.02	3.1	0.0586	0.0054	1.01
O 141 m	40.1	0.0586	0.0084	1.03	—	—	—	—
O 243 m	18.6	0.0625	0.0082	1.02	—	—	—	—
O 371 m	16.5	0.0586	0.0097	1.03	—	—	—	—
P 64 m	—	—	—	—	13.7	0.0625	0.0100	1.06
					2.3	0.0508	0.0108	1.51
P 164 m	—	—	—	—	8.8	0.0625	0.0074	1.03
P 261 m	—	—	—	—	2.2	0.0625	0.0097	1.20
E 23 m	25.8	0.0664	0.0122	1.10	4.4	0.0625	0.0099	1.46
					3.4	0.0508	0.0118	7.02
E 49 m	9.9	0.0625	0.0107	1.18	1.4	0.0547	0.0156	1.41
E 89 m	13.2	0.0625	0.0069	1.03	5.7	0.0586	0.0069	1.22

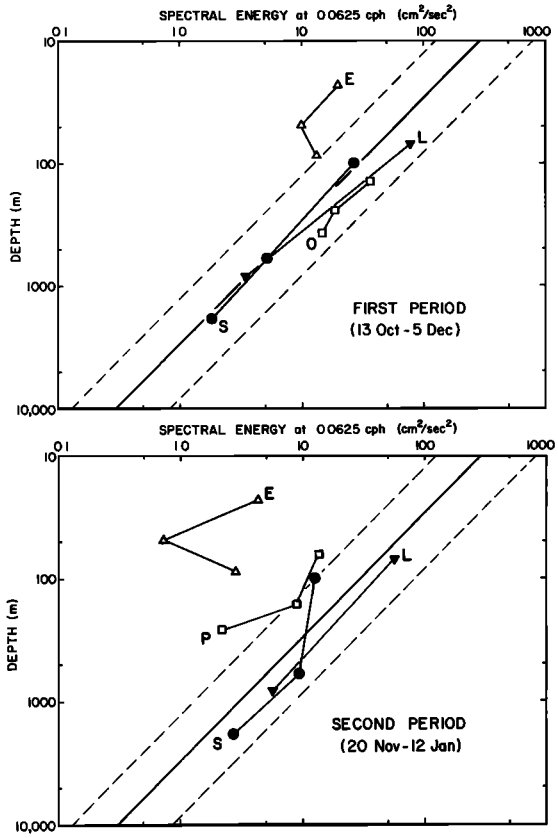

Fig. 6. Log-log plot of the clockwise spectral energy versus depth for both time periods. Along the solid line energy would vary inversely with depth. The separation between the dashed lines indicates the 95% confidence interval for each spectral estimate.

spectra [*Mooers*, 1973] shows that the near-inertial motion is very nearly circular offshore, with slight ellipticity over the continental shelf (Table 1). The bandwidth of the near-inertial peak, defined as the difference between frequencies where the energy falls to one-half of the peak value [*Fu*, 1981], is about 0.008 cph (twice the spectral bandwidth) offshore, and somewhat greater over the continental shelf (Table 1). The bandwidth of the peak is inversely proportional to the persistence of near-inertial motions [*Munk and Phillips*, 1968]; the persistence seems to be about 120 hours offshore and 100 hours over the shelf.

During the second period, there were prominent near-inertial peaks at all current meters of the three offshore moorings (Skunk, Leopard, and Puma), similar to those observed during the first time period, except that the energy was generally lower and the bandwidth was generally greater (Table 1). Over the continental shelf, the inertial energy was much smaller during the second time period than during the first (Table 1, Figure 5). The spectrum of the top current meter at Elephant (Figure 5) has two near-inertial peaks, centered at 0.0625 cph (very near f) and 0.0508 cph (about 14% below f), respectively. A similar split was observed at Puma 64, near the shelf edge (Table 1). Elephant 49 m has a relatively broad, flat peak centered at 0.0547 cph, about 7% below f. All other current meters have a single peak frequency that is very nearly equal to f or somewhat greater than f (Table 1). The downward frequency shifts may be a result of Doppler shifting of the near-inertial motion in the presence of a mean flow [*Thomson and Huggett*, 1981]: There was strong mean alongshore flow, about 20–30 cm/s, at Elephant 23 m, Elephant 49 m, and Puma 64 during the second period; elsewhere the mean flow was much weaker. During the first period, mean currents were weak everywhere.

During both time periods, the near-inertial energy decreases monotonically with depth at each of the offshore moorings (Table 1). A log-log plot of the energy versus depth at the most common peak frequency (Figure 6) shows that the points from Skunk, Leopard, and Ocelot lie roughly along a straight line corresponding to an inverse relationship between energy and depth. During both time periods the current meters at Elephant (i.e., over the shelf) have much less near-inertial energy than offshore current meters at the same depth (Figure 6). The current meters at Puma, at the edge of the continental shelf, have less near-inertial energy than those in the deep water but more than those over the shelf (Figure 6). Data from previous studies show a similar variation of near-inertial energy with depth. The energy levels observed in the open North Atlantic [*Pollard*, 1980; *Fu*, 1981] seem to be comparable to those at Skunk, Leopard, and Ocelot (i.e., these data seem roughly to obey the same inverse relationship between energy and depth). The near-inertial energy observed over the Oregon shelf in summer 1973 [*Kundu*, 1976] are similar to those at Elephant, and energy levels from the vicinity of the 200-m isobath in Queen Charlotte Sound [*Thomson and Huggett*, 1981] are comparable to those at Puma. Thus, it may be generally true that there is less near-inertial energy over the continental shelf than at similar depths in the open ocean.

Coherence and phase spectra were computed for all current meter pairs and both time periods. With 10 degrees of freedom, coherence squared values of 0.53, 0.58, and 0.68 are significantly different from zero at the 95, 97, and 99% levels, respectively [*Thompson*, 1979]. There was significant coherence at the 95% level at a clockwise-rotating frequency between 0.0508 and 0.0664 cph between 23 out of 55 current meter pairs during the first period and between 19 pairs during the second period. During both periods, there was generally higher coherence between horizontally or diagonally separated current meters than between vertically separated current meters (Figure 7).

The horizontal coherence scale exceeded the extent of the array (115 km) during the first period and was at least half the extent of the array during the second period (Figure 8). The large horizontal coherence scale of the first period exceeds those observed in the open ocean at comparable depths [*Fu*, 1981] and is comparable to the coherence scales observed in the surface mixed layer at site D in the North Atlantic [*Pollard*, 1980] and in the relatively shallow waters of Queen Charlotte Sound off British Columbia [*Thomson and Huggett*, 1981].

Phase spectra were also computed for both time periods, and confidence limits for phase were determined by the procedure described by *Koopmans* [1974, p. 284–285]. This method of computing confidence intervals is conservative, since it assumes that the time series data have a Gaussian distribution; if one assumes instead that the data consists of a coherent signal plus incoherent noise, the phase estimates would be exact [*Schott and Düing*, 1976]. The phase differences between current meter pairs can be used to determine the direction of phase propagation and the wavelength of the motion, if the separation between current meters (horizontally or vertically) is small compared with the wavelength of the near-inertial motions. For example, *Kundu* [1976] used data from 11 current meters separated vertically by 4–20 m to estimate upward phase propagation of 0.1–0.4 cm s^{-1} and vertical wavelengths of 55–225 m. In our case, most of the current meter separations are diagonal, making it difficult to estimate either the vertical or horizontal propagation speeds. To add to the difficulty, most of the sepa-

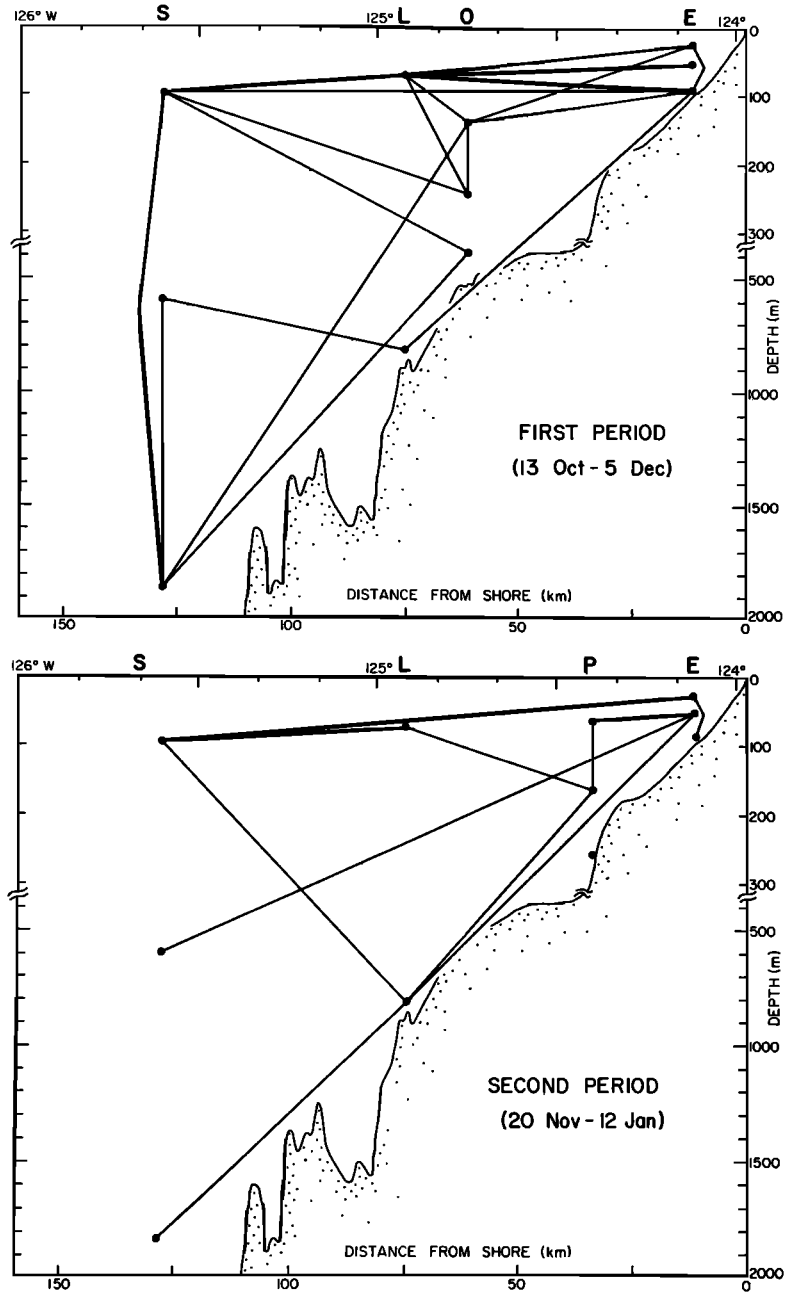

Fig. 7. Distribution of current meter pairs coherent in the clockwise rotating inertial frequency band of 0.0508–0.0664 cph. Pairs connected by solid lines have a squared coherence of at least 0.58, the 97% significance level.

rations (both vertical and horizontal) are larger than the expected vertical and horizontal wavelengths. Nevertheless, we used the phase spectra to estimate the horizontal east-west (cross-shelf) wavelength by making the following assumptions: (1) phase propagation was from east to west (i.e., energy propagated onshore); (2) the vertical separation (maximum of 71 m) between Elephant 89 m, Puma 64 m, Ocelot 141 m, Leopard 70 m, and Skunk 100 m was insignificant when compared with the horizontal separation; (3) during the first period, the horizontal wavelength was larger than the smallest horizontal separation; and (4) during the second period, the horizontal wavelength was slightly smaller than the smallest separation. With these assumptions, the phase difference of 115° between Leopard 70 m and Ocelot 141 m (13.9 km apart) during the first period yields an east-west wavelength of 44 km with an 80% confidence interval of 36–56 km. Similarly, the phase difference of 380° (20° + 360°) between Puma and Elephant (19.7 km apart) yields a wavelength of 19 km (the 80% confidence interval is 18–20 km). By adding integral numbers of 360° to the phase differences between the other pairs, we were able to obtain consistent estimates of the cross-shelf wavelength for each time period (Table 2). The average wavelength obtained was 50 km for the first period and 20 km for the second period. The 50-km wavelength for the first period is consistent with the large coherence scale observed then: Only three wavelengths span the entire array. During the second period, both the estimated wavelength and the coherence scale are shorter. In both periods, there is significant coherence between current meters separated by two horizontal wavelengths or less.

We also considered estimating the vertical wavelength, but

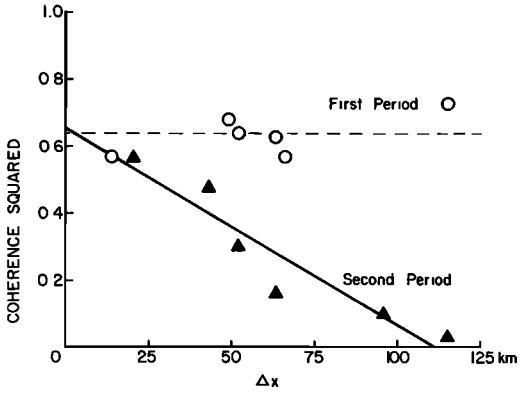

Fig. 8. The squared coherence at 0.0625 cph between pairs of current meters with roughly horizontal separation: Skunk 100 m, Leopard 70 m, Ocelot 141 m, Puma 64 m, and Elephant 89 m. The 90%, 95%, and 97% significance levels are 0.44, 0.53, and 0.58, respectively.

there was significant coherence between only a few vertically separated pairs. The spacing of the current meters was too large to resolve vertical wavelengths of the magnitude (50–500 m) generally observed in the ocean. Although we could have obtained estimates by assuming particular values of integral wavelengths between current meters, the choice would have been completely arbitrary, and, hence, the resulting estimates would be meaningless.

BAND-PASSED DATA

To examine the time variability of the near-inertial motion, we followed *Kundu*'s [1976] example and used the technique of band-passing rather than complex demodulation. (While the latter has the advantage of using both components of the original vector time series, the former has the advantage of showing the current variability more clearly. In a case like ours, where the motion in the near-inertial frequency band is essentially circular and clockwise, the two techniques give equivalent results.) The current records were band passed by using a narrow filter centered at 0.0625 cph, the most common frequency of the near-inertial peak in the autospectra. The procedure was to determine the Fourier components of each current record by using a Sande-Tukey fast Fourier transform, pass 100% of the energy in the frequency band between 0.050 and 0.075 cph, and suppress all of the energy at frequencies less than 0.048 cph and greater than 0.077 cph, tapering linearly within the edges (0.002 cph wide) of the filter. The band passed by the filter lies entirely between the semidiurnal and the diurnal tidal frequencies. For computational efficiency, we filtered only 2048 hours of the long records, 1408 hours of the Ocelot records, and 1280 hours of the Puma records. In each case, there were at least 32 Fourier components within the band passed by the filter.

The possibility of peak smearing due to the sharp filtering was tested by using a synthetic 1024-hour series with 5, 10, or 15 cycles of motion at 0.0625 cph, with the remainder of the series set to zero. Like *Kundu* [1976], we found that peak smearing is less pronounced when the number of cycles was greater: When the input series contained more than 10 cycles, the amplitude of the band-passed output did not vary greatly from the input series. The phase of the near-inertial motion was not altered by the band-pass filter, regardless of the number of cycles.

The time series of the eastward component of the band-passed current at all current meters (Figure 9) shows there is some near-inertial motion throughout most of each record. The energy seems to occur predominantly in bursts or 'events' of several days duration. Some of these events appear to begin impulsively and decay gradually, but others increase gradually and persist for more than a week. The maximum value (39 cm/s) of the band-passed data occurred at Leopard 70 at the end of October. At each current meter, the band-passed northward current is very similar to the eastward component, except that it is 90° out of phase (e.g., Figure 10).

The time series of the band-passed data (Figure 9) demonstrate explicitly some of the conclusions drawn from the spectral analysis: The strongest near-inertial currents occur at the offshore moorings, and at each location the amplitude generally decreases with depth. During the first period, October 13 to December 5, the near-inertial motion is very persistent at the offshore moorings and less persistent over the continental shelf. At most current meters, the largest amplitudes occur during the first period rather than the second. During the second time period, November 20 to January 12, there is very little near-inertial energy over the continental shelf.

During each period of high near-inertial energy, the phase difference between the band-passed current vectors at Skunk 100 m and Leopard 70 m, and between Leopard 70, and Ocelot 141 m, remained fairly constant (Figure 11). During the strong near-inertial event of October 27 to November 13, Skunk 100

TABLE 2. Horizontal East-West (Cross-Shelf) Wavelengths Calculated From Phase Differences at 0.0625 cph, for Current Meter Pairs With Nearly Horizontal Separations.

	First Period (Oct. 13 to Dec. 5)					Second Period (Nov. 20 to Jan. 12)			
Current Meter Pairs	Separation Distance, km	Coherence Squared	Phase Difference	*N*	Wavelength, km	Coherence Squared	Phase Difference	*N*	Wavelength, km
S 100–L 70	52.3	0.64	331° ± 21°	0	57	0.30	163° ± 49°	2	21
S 100–O 141	66.4	0.57	78° ± 25°	1	55	—	—	—	—
S 100–P 64	95.6	—	—	—	—	0.10	—	—	—
S 100–E 89	115.3	0.73	91° ± 17°	2	50	0.03	—	—	—
L 70–O 141	13.9	0.57	115° ± 25°	0	44	—	—	—	—
L 70–P 64	43.1	—	—	—	—	0.48	21° ± 31°	2	21
L 70–E 89	62.8	0.63	128° ± 22°	1	46	0.16	—	—	—
O 141–E 89	48.9	0.68	25° ± 20°	1	46	—	—	—	—
P 64–E 89	19.7	—	—	—	—	0.57	20° ± 25°	1	19

The 80% confidence interval is shown for phase; *N* is the assumed number of integral wavelengths between each pair.

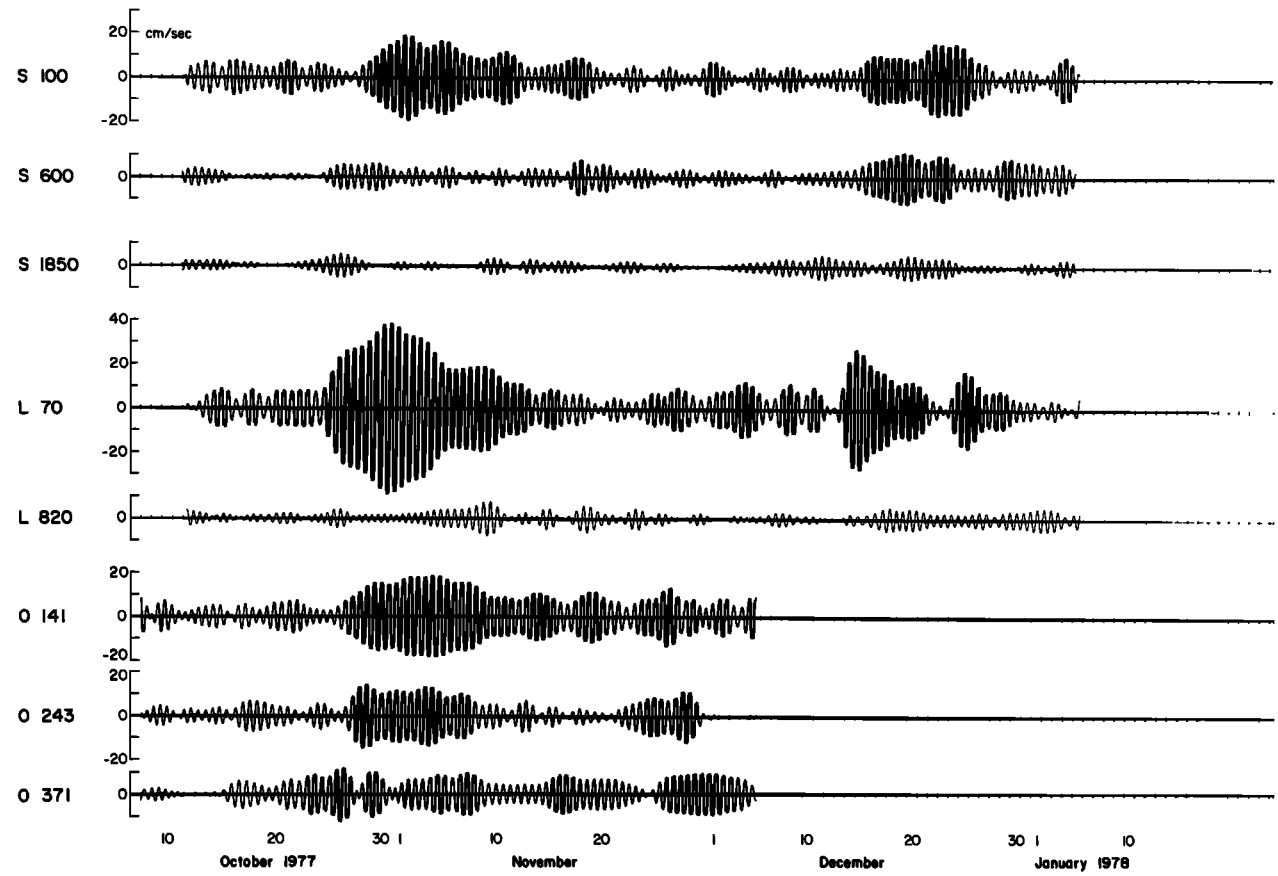

Fig. 9*a*

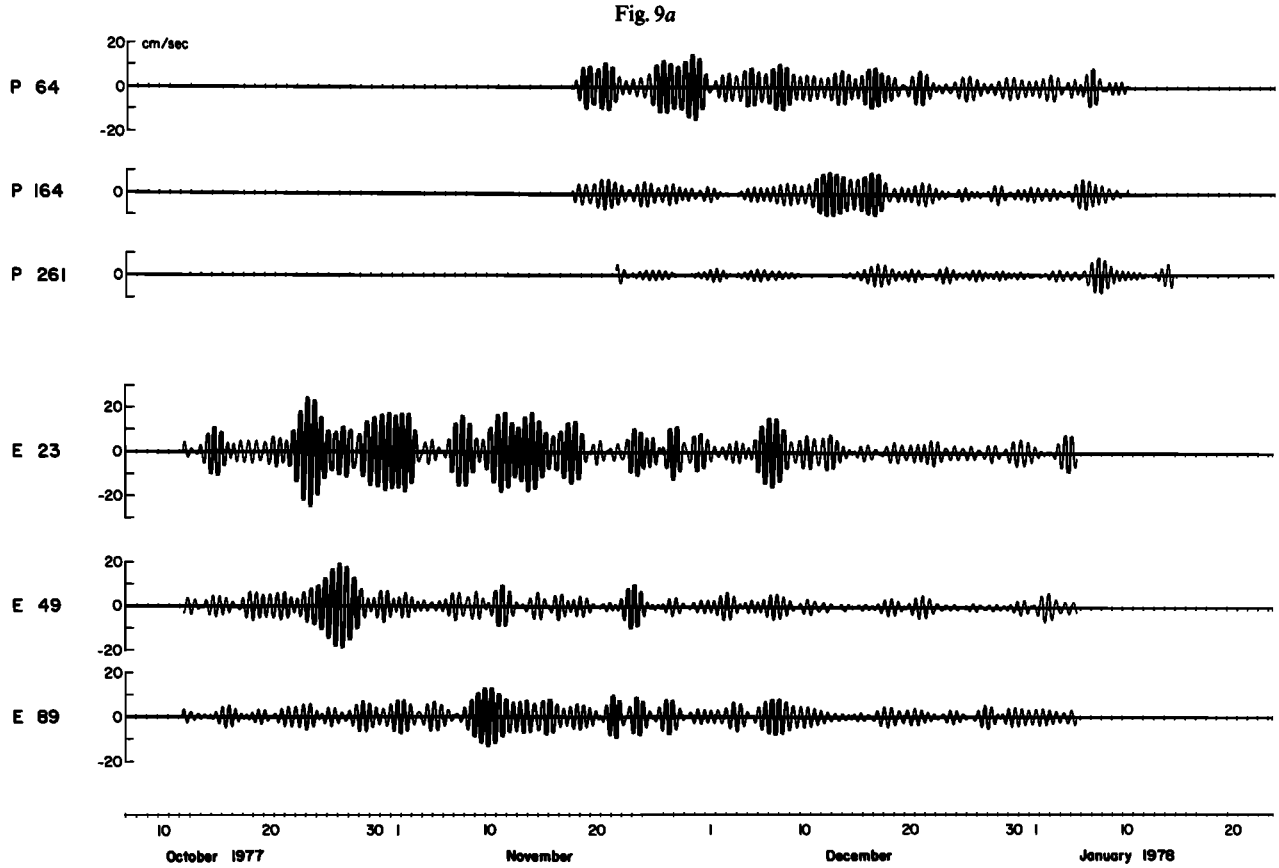

Fig. 9*b*

Fig. 9. The band-passed time series of the eastward component of the current at the current meters at (*a*) Skunk, Leopard, and Ocelot, and (*b*) Puma and Elephant.

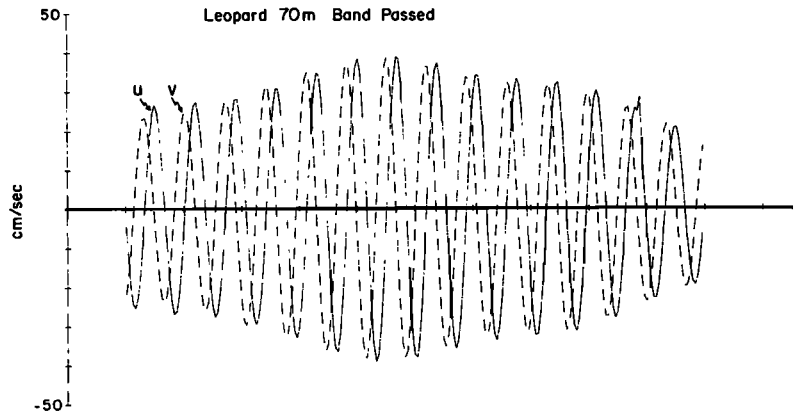

Fig. 10. A 10 day (Oct. 27 to Nov. 6) segment of the band-passed eastward (u) and northward (v) components of current at Leopard 70 m. The approximately equal amplitude of the components and the 90° lag of u behind v indicate clockwise circular motion.

m lags behind Leopard 70 m by about 330°, and Leopard 70 m lags behind Ocelot 141 m by about 120°; these numbers agree very well with the phase spectra for the first period (Table 2). Thus, the horizontal wavelength estimate of 50 km seems to be valid throughout the 20-day duration of strong near-inertial motion beginning about October 27.

Several current meters showed high near-inertial energy during December 13–28 (Figure 9). At Leopard 70 m, there seem to be two separate near-inertial events that begin about December 13 and December 24; the near-inertial energy at Skunk 100 m seems to be more nearly continuous. The phase difference between Skunk 100 m and Leopard 70 m varies considerably during this period: It is about 180° on December 14–16, about 75° on December 18–22, and about 270° on December 24–28; only the first of these agrees well with phase spectra for the second period (Table 2). Thus, the near-inertial phase difference between a pair of current meters seems to be well defined and fairly constant during a particular near-inertial event but varies considerably from one event to another. To the extent that differences in phase reflect different

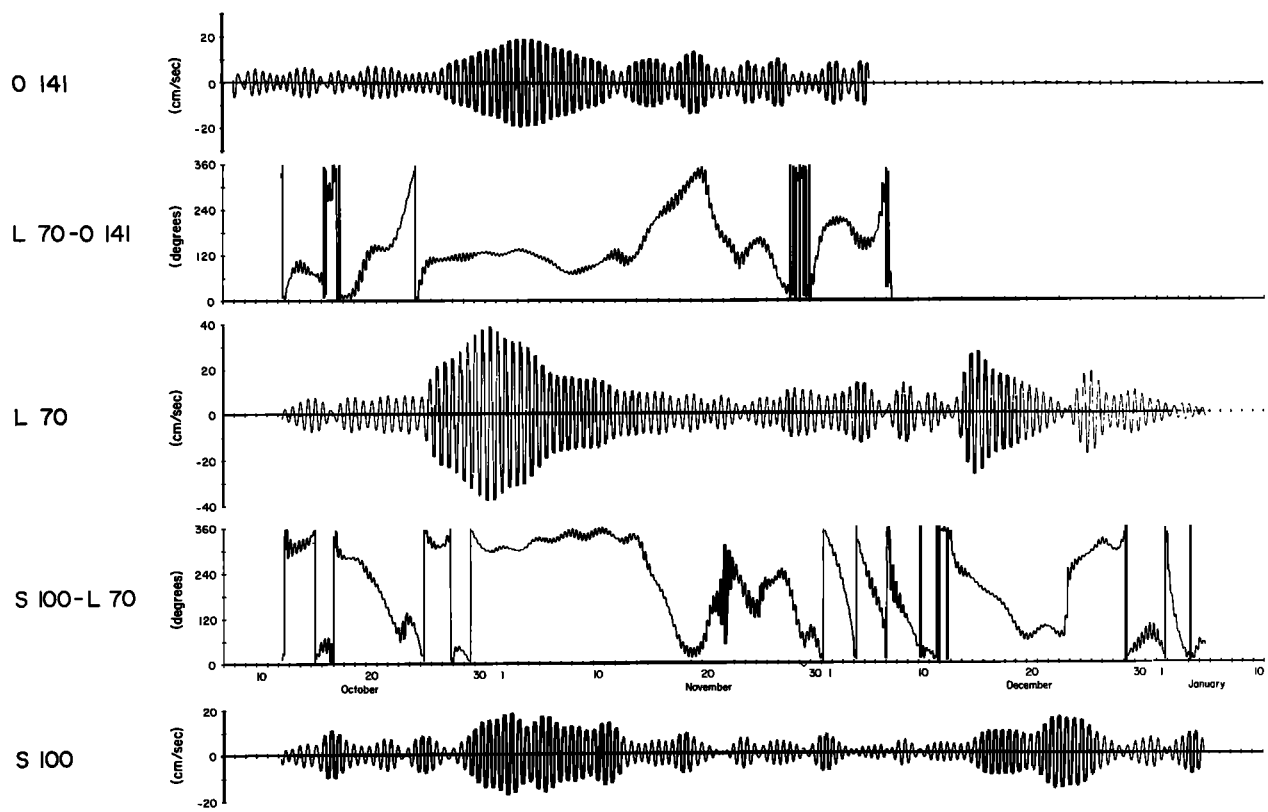

Fig. 11. The hourly difference in direction between the Leopard 70 m and the Skunk 100 m or Ocelot 141 band-passed current vectors.

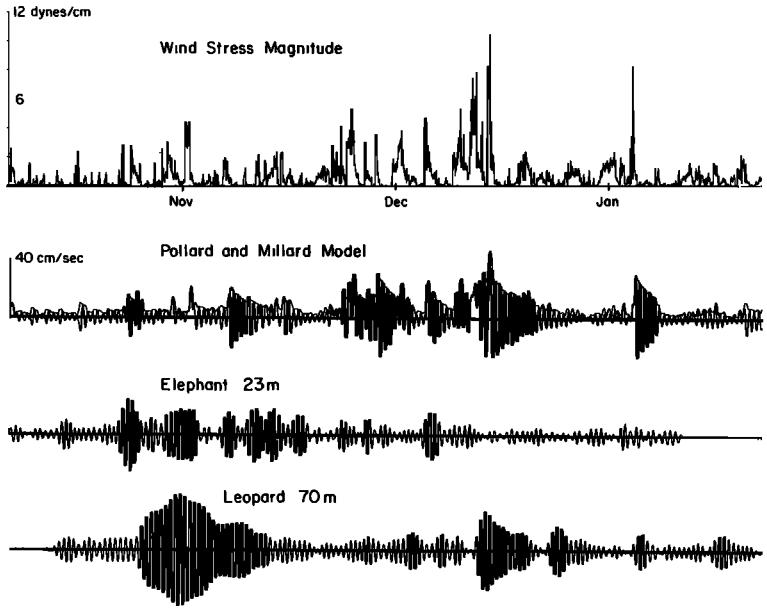

Fig. 12. The magnitude of the Newport wind stress, and the magnitude and eastward component of the Pollard and Millard model, and eastward components of the band-passed current at Elephant 23 m (in the mixed layer), and Leopard 70 m (about 30 m below the mixed layer).

wavelengths, these variations imply that the wavelength of near-inertial motions varies considerably between different energetic episodes.

WIND FORCING

The generation of near-inertial motion in the mixed layer by local wind forcing at site D in the North Atlantic was modeled successfully by *Pollard and Millard* [1970]. Although most of our current observations were well below the mixed layer and the nearest wind observations were made on the Newport south jetty 85 km south of the array, we used the Pollard and Millard model to obtain a qualitative estimate of the currents that might have been generated by the observed winds. The model equations are

$$u_t - fv = \tau^x/(\rho Z) - cu \quad (1)$$

$$v_t + fu = \tau^y/(\rho Z) - cv \quad (2)$$

where f is the local inertial frequency, u and v are eastward and northward components of the current, c is the damping coefficient, ρ is the water density, $\tau(\tau^x, \tau^y)$ is the wind stress, and Z is the mixed layer depth. The wind stress, $\tau = C_d\rho_a |\mathbf{V}|\mathbf{V}$, was computed from the Newport hourly vector, V, the density of air, $\rho_a = 1.25 \times 10^{-3}$ gm/cm^3, and a drag coefficient, $C_d = 1.5 \times 10^{-3}$. We assumed a constant mixed layer depth of 25 m. We used a simple finite difference form with a 4-s time step to compute hourly values of the model current.

The Pollard and Millard model shows a strong near-inertial response to the wind stress peaks of December 14 and January 4 (Figure 12), and a weaker response to some of the weaker storms between November 7 and December 10. Near-inertial motion was observed more frequently at Leopard 70 m than in the Pollard and Millard model results (Figure 12). Near-inertial motion occurred frequently at Elephant 23 m from mid-October to early December, but not immediately after the strong storms of December 14 and January 4, although both of these storms seemed to generate near-inertial motions at Leopard 70 m. The model failed to account for the persistent and energetic near-inertial motion observed at the three offshore moorings in late October and early November. Since the model is very sensitive to small-scale variations in the wind field [*Pollard*, 1980], we might expect poor agreement between observed currents and model results whenever there are strong atmospheric fronts in the region.

Frontal passages were very common off Oregon during late October and early November (Figure 13): between October 23 and November 15, 17 fronts associated with low pressure centers of varying size and intensity passed eastward over the SUS array. Many of these frontal passages were recorded in the Newport pressure data and caused clockwise rotation of the wind at Newport (Figure 13). Since the extent of the SUS array was 115 km, the arrival time of each front would not generally be the same time at all moorings. Wherever the rotation of the near-inertial motion caused by each frontal passage was in phase with the pre-existing near-inertial motion, there would be constructive interference [*Pollard*, 1970] which would increase the near-inertial energy. To look for phase shifts in the observed near-inertial motion, we calculated the phase difference between the band-passed current vectors and a reference vector rotating clockwise at 0.0625 cph: vectors with no phase shifts will have a constant phase difference if they have the same frequency as the reference vector or a linearly increasing and decreasing phase difference if their frequency is slightly different. Time series of this phase difference for Leopard 70 m and Elephant 23 m (Figure 13) show that no shifts in the phase of the near-inertial motion occurred at Leopard 70 m during late October/early November, while several phase shifts occurred at Elephant 23 during the same period. This suggests that most of the wind-generated near-inertial motion at Leopard in late October/early November was nearly in phase, causing the strong persistent near-inertial currents there. On the other hand, some of the near-inertial motion generated at Elephant may have been out of phase with pre-existing near-inertial motions, causing destructive interference on about October 27 and again on November 4 and 6. Thus, the observations strongly suggest that the strong and persistent near-inertial

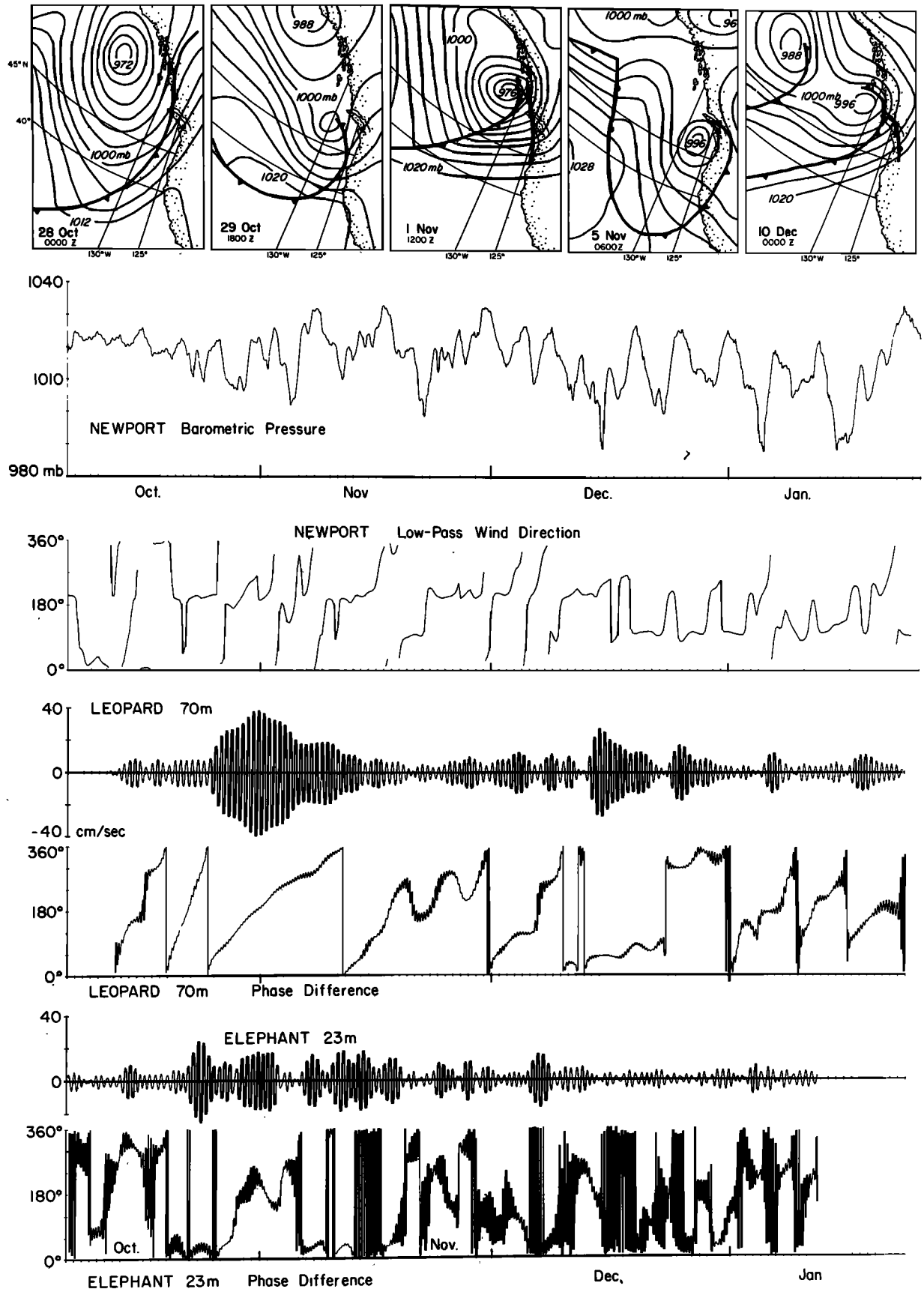

Fig. 13. Examples of the synoptic atmospheric pressure charts from the period of the near-inertial 'event' of late October/early November and time series of atmospheric pressure and the direction of the low-passed (<0.025 cph) wind at Newport, with the eastward components and the phase differences of the band-passed current vectors at Leopard 70 m and Elephant 23 m relative to a reference vector rotating clockwise at 0.0625 cph.

motions observed at the offshore moorings in late October and early November were generated by the local wind. Without direct wind observations over the moorings, this tentative conclusion cannot be verified.

CONCLUSIONS

Near-inertial motions were observed at all current meters in an array of five moorings which spanned the continental margin off Oregon between October 1977 and January 1978. The current meters were between 23 and 1850 m deep, in water depths between 100 and 2500 m, at locations between 10 and 130 km from shore. Although almost all of the current meters were below the mixed layer, large amplitude ($\sim$20 cm/s) near-inertial motions were observed on several occasions. The largest amplitude (>30 cm/s) near-inertial motions were observed at the shallowest current meters of the offshore moorings; these current meters were in the pycnocline at depths between 70 and 141 m. Although there were current meters at shallower depths (23 and 49 m) within the surface mixed layer over the continental shelf, there was much less near-inertial energy there. The amount of near-inertial energy observed over the shelf was similar to that observed there in the summer of 1972, and the amount of energy in the deep water was comparable to that observed in the North Atlantic.

Most of the near-inertial motion had a frequency slightly greater than the local inertial frequency, but some of it had a frequency less than the local inertial frequency. The downward frequency shift occurred in the presence of a strong northward current.

The near-inertial motion at some current meters was very persistent (in one case it persisted for more than 15 days). In this case, the amplitude seemed to increase gradually before it decayed. In other cases, the amplitude increased impulsively with gradual decay, as usually observed elsewhere.

Spectral analysis showed that the horizontal coherence scale exceeded the extent of the array (115 km) in October and November and was about half the extent of the array (i.e., 60 km) in December and early January. These coherence scales are much larger than those previously observed over the Oregon shelf in summer. Estimates of the horizontal wavelength of the motion changed from 50 km during the first half of the records to about 20 km during the second. These estimates suggest that there is significant coherence between current meters separated by two wavelengths or less.

The near-inertial phase difference between a pair of current meters varied considerably between separate near-inertial events, even though the stratification remained much the same throughout the period of observation. This suggests that the wavelength is the result of the particular circumstances generating the motion, rather than of the oceanic environment.

Because of the lack of current measurements in the mixed layer and the absence of direct wind measurements over each mooring, we could not rigorously test the hypothesis of local generation of the near-inertial motions. However, the simple Pollard and Millard model of local forcing, using the Newport wind observations (85 km south of the array) as the forcing function, indicates that some of the near-inertial motion observed below the mixed layer (e.g., at Leopard 70 m) was generated impulsively by strong peaks in the wind stress (e.g., December 14 and January 4). The strong and persistent period of near-inertial motion in late October and early November may have been the result of a sequence of fronts that happened to pass over the region in the proper phase for constructive interference. Thus, our data are consistent with the hypothesis that the local wind can force strong near-inertial motions at depths well below the mixed layer.

Acknowledgments. We wish to thank Barbara Hickey of the University of Washington for providing the data at Ocelot and Elephant. We also thank Rick Romea and Jim Richman for their comments on earlier drafts and Joseph Bottero and William Gilbert for assistance in the analysis. This study was completed while the first author was studying for a degree at Oregon State University. Financial support was provided by the United States Coast Guard and by the National Science Foundation through grants OCE-7925019 and OCE-8026131.

REFERENCES

Fu, L., Observations and models of inertial waves in the deep ocean, *Rev. Geophys. Space Phys.*, *19*, 141–170, 1981.

Gonella, J., A local study of inertial oscillations in the upper layers of the ocean, *Deep Sea Res.*, *18*, 775–788, 1971.

Johnson, W., Cyclesonde measurements in the upwelling region off Oregon, *Tech. Rep. 76-1*, Rosential School of Mar. and Atmos. Sci., Univ. of Miami Florida, 1976.

Kindle, J. C., The horizontal coherence of inertial oscillations in a coastal region, *Geophys. Res. Lett.*, *1*, 127–130, 1974.

Koopmans, L. H., *The Spectral Analysis of Time Series*, Academic, New York, 1974.

Kroll, J., The propagation of wind-generated inertial oscillations from the surface into the deep ocean, *J. Mar. Res.*, *33*, 15–51, 1975.

Kundu, P. K., An analysis of inertial oscillations observed near the Oregon coast, *J. Phys. Oceanogr.*, *6*, 879–898, 1976.

Mooers, C. N. K., A technique for the cross spectrum analysis of pairs of complex-valued time series, with emphasis on properties of polarized components and rotational invariants, *Deep Sea Res.*, *20*, 1129–1141, 1973.

Munk, W., and N. Phillips, Coherence and band structure of inertial motion in the sea, *Rev. Geophys.*, *6*, 447–471, 1968.

Pollard, R. T., On the generation by winds of inertial waves in the ocean, *Deep Sea Res.*, *17*, 795–812, 1970.

Pollard, R. T., Properties of near-surface inertial oscillations, *J. Phys. Oceanogr.*, *10*, 385–398, 1980.

Pollard, R. T., and R. C. Millard, Comparison between observed and simulated inertial oscillations, *Deep Sea Res.*, *17*, 815–821, 1970.

Schott, F., and W. Düing, Continental shelf waves in the Florida Straits, *J. Phys. Oceanogr.*, *6*, 451–460, 1976.

Thompson, R. O. R. Y., Coherence significance levels, *J. Atmos. Sci.*, *36*, 2020–2021, 1979.

Thomson, R. E., and W. E. Huggett, Wind driven inertial oscillations of large spatial coherence, *Atmos. Ocean*, *19*, 291–306, 1981.

Webster, F., Observations of inertial-period motions in the deep sea, *Rev. Geophys.*, *6*, 473–490, 1968.

(Received July 6, 1982;
revised January 31, 1983;
accepted March 21, 1983.)